

# Preparation and characterization of microcrystalline Si and Ge thin films

J. González-Hernández

*Depto. de Física, Centro de Investigación y Estudios Avanzados,  
Instituto Politécnico Nacional, Apartado postal 14-740, 07000 México, D.F.*

(Recibido el 7 de septiembre de 1987; aceptado el 19 de julio de 1989)

**Abstract.** Preparation and characterization of microcrystalline silicon and germanium thin films are discussed. Several characterization techniques, such as electrical measurements, Raman spectroscopy, transmission electron microscopy, X-Ray diffraction and scanning electron microscopy have been used for the present study. In particular, electrical conductivity percolation and grain-size measurements are discussed. The single most important effect on the properties of microcrystalline Si and Ge is the presence of impurities. Thus, better technical performance must be preceded by an improvement in vacuum and purer gases used in the deposition systems.

**PACS:** 73.60.-n; 73.60.Aq

## 1. Introduction

In the past few years, considerable interest has developed in the preparation of microcrystalline and polycrystalline silicon and germanium thin films for various applications. For instance, microcrystalline Si has been successfully used as a substrate semiconductor for thin-film transistors applied to large area flat panel displays [1,2].

Polycrystalline solids are usually grown from the melt or from solutions resulting in bulk forms, while microcrystalline solids are generally in the form of films prepared by vapor condensation or crystallization from the amorphous phase. In this work we shall deal with the formation of both microcrystalline silicon and germanium either by direct deposition or by annealing of deposited films in the amorphous phase. We shall treat in some detail grain-size,  $L$ , crystallization temperature,  $T_c$ , of as-deposited amorphous films and the temperature of the substrate separating the amorphous from the microcrystalline phase. The results of this study suggest that the presence of residual contamination plays an important role to determine the physical properties of the silicon and germanium films.

## 2. Sample preparation

The microcrystalline Si and Ge films were prepared using a Perkin Elmers molecular beam deposition (MBD) system with a base pressure in its deposition chamber in

the low  $10^{-10}$  Torr. The samples were deposited on various types of substrates and over a wide range of substrate temperature. Under those conditions films with crystal structures from completely amorphous to highly crystalline were produced. Deposition rates of a few Amstrongs per second are typical in MBD systems, the total nominal thickness of most of the films analyzed in this study was of one micrometer.

### 3. Results and discussions

#### A. Raman scattering

Raman Scattering is an extremely useful technique to characterize the structure of materials via the dynamic properties of the phonon modes. This technique is a very convenient and quick tool to distinguish an amorphous phase from a crystalline phase. It can be applied to any material in the bulk or thin film form on any type of substrate. Due to the lack of translational symmetry, in the former phase, crystal momentum is not conserved resulting in a Raman spectrum similar to the crystalline phonon density of states with an optical peak at  $460\text{--}480\text{ cm}^{-1}$  for the case of silicon, depending on preparation conditions. The momentum conservation dictates a sharp peak from the zone-center phonons located at  $500\text{--}522\text{ cm}^{-1}$  depending on the grain-size, with the partial restoration of translational symmetry in microcrystalline silicon. The grain size dependence comes from the  $KL = 1$  rule (Heisenberg uncertainty principle)  $L$  being the average particle size. Because the phonon dispersion relations for silicon has a maximum at  $522\text{ cm}^{-1}$  at  $K = 0$ , the frequency of the phonon at  $K = L^{-1}$  is lowered. Thus the particle size  $L$  may be determined from the position of this peak given the phonon dispersion relations. Following the method proposed by Richter *et al.* [3] the average grain size was determined from the details of the Raman line. Fig. 1 shows a typical series of spectra for microcrystalline silicon having various particle sizes. Sample 101 having a peak at  $508\text{ cm}^{-1}$  corresponds to  $L = 20\text{ \AA}$  while sample 088 is amorphous. Crystalline Si having  $L$  greater than  $100\text{ \AA}$  exhibits a peak near  $522\text{ cm}^{-1}$  at room temperature, the same peak position is observed for a single crystal. Thus, Raman scattering can not be applied in the analysis of microcrystallinity in samples where grain size is larger than  $100\text{ \AA}$ . Notice that the microcrystallinity also results in an asymmetric broadening of the Raman peak.

#### B. Percolation in conductivity

The presence in percolation processes of a sharp phase transition at which long-range connectivity abruptly appears, provides a well defined model for the study of spatially random phenomena in mixed systems [4].

The critical volume fraction of crystallinity,  $X_c$  at the onset of conduction in a percolation process has been experimentally determined for a system of microcrystalline Si embedded in an a-Si matrix. Highly phosphorus doped amorphous

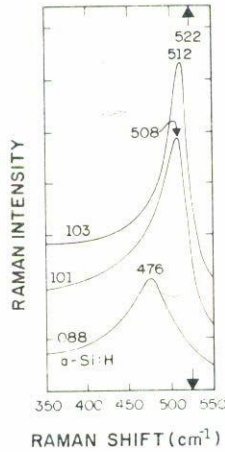


FIGURE 1. Raman spectra for microcrystalline silicon having various particles size. The bottom curve is a typical Raman spectrum from hydrogenated amorphous silicon.

silicon alloys prepared by glow-discharge of  $\text{SiF}_4/\text{H}_2$  have been found to contain microcrystallinity. Samples having a volume fraction,  $X$ , of microcrystallinity in a wide range were analyzed by Raman and electrical measurements. Fig. 2 shows a typical Raman spectrum of a sample having  $X = 0.22$ . The experimental curve (continuous line) has been resolved into two parts:  $I_a$ , shaded; and  $I_c$ . In order to decompose the total Raman intensity, a computer program was used to fit a typical amorphous spectrum to the lower energy side of the measured spectrum where no contribution from the crystalline component is expected. The maximum of the amorphous component is located at  $480 \text{ cm}^{-1}$ . After subtracting  $I_a$  from the total measured scattering the remaining area under the curve is attributed to  $I_c$ , the contribution from the fraction of crystallinity.

Let us define  $X$  by

$$X = \frac{I_c}{I_c + I_a}, \quad (1)$$

in which  $I_c = \Sigma_c X$  and  $I_a = \Sigma_a(1 - X)$ , where  $\Sigma$  is the integrated backscattering cross section over the measured frequency range. Solving Eq.(1) for the volume fraction of crystallinity,  $X$

$$X = \frac{X}{X + y(1 - X)}, \quad (2)$$

where  $y = \Sigma_c/\Sigma_a$  is the ratio of the integrated Raman cross section for c-Si and a-Si. In order to find  $y$ , two standard samples were prepared: one shows only the amorphous part and the other shows only the crystalline part. Since  $I = \Sigma v$ , with

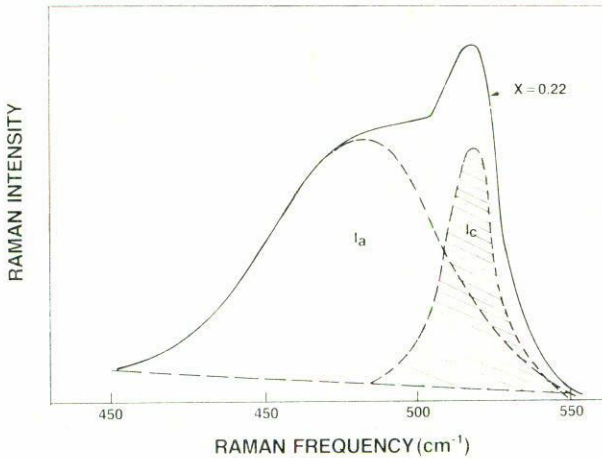


FIGURE 2. Raman spectrum of a Silicon film having a mixture of amorphous ( $I_a$ ) and crystalline ( $I_c$ ) phases. For this sample the calculated volume fraction of crystallinity  $X_c = 0.22$ .

$v$  being the scattering volume, the ratio  $y$  may be expressed by  $y = I_c \alpha_c / \alpha_a$ , where  $\alpha_c = 1.34 \times 10^5 \text{ cm}^{-1}$  and  $\alpha_a = 1.68 \times 10^5 \text{ cm}^{-1}$  are the measured absorption coefficients at 2.5 eV energy of the excitation source for the microcrystalline and amorphous samples respectively.

In Fig. 3 we show the measured conductivity versus the calculated volume fraction  $X$ . For  $X < 0.16$ , the conductivity is nearly constant, being approximately  $10^{-4} (\Omega \text{ cm})^{-1}$ , typical of phosphorus-doped a-Si:H. However, for  $X \geq 0.16$ , the conductivity increases exponentially and shows saturation for higher  $X$  values. Also shown in Fig. 3 is the  $\phi_c(3D) = 0.16$  for Zallen's [4] latest calculation of the threshold value for percolation in a three dimensional system. In order to corroborate that the sample structure agrees with Zallen's predictions, the films were analyzed by TEM. It was found that the crystalline component consist of small crystallites having an approximately round shape and isotropically distributed throughout the film volume. Thus, as far as the conductivity measurements is concerned, the system is an isotropic three dimensional system.

Zallen [4] also found that for a system with lower dimensionality  $X_c$  is larger. In fact, for a system with only one dimension (a wire),  $X_c = 1$ . For an isotropic two dimensional system he found an intermediate value for  $X_c = 0.45$ . To my knowledge, no experimental work supporting Zallen's result for percolation conductivity in a two dimensional system has been reported so far.

In the present work, Raman spectroscopy and conductivity studies have been extended to germanium films. In this case two critical values were obtained for films prepared under different substrate temperatures. Subsequent structural investigations using scanning electron microscopy (SEM) cross-section revealed that a higher value of  $X_c \sim 0.4$  belonged to a group of films all showing columnar structure and a lower value of 0.15 belonged to those having crystallites with spherical shape.

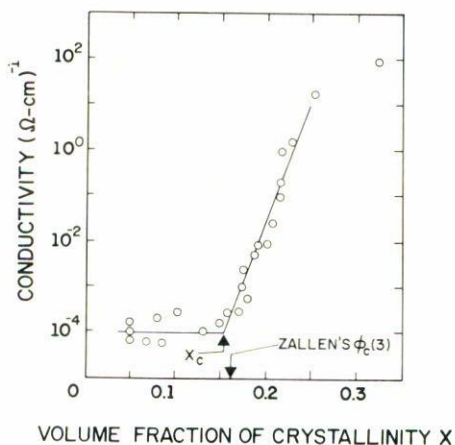


FIGURE 3. Electrical conductivity versus volume fraction of crystallinity. The threshold value for percolation,  $\phi_c(3)$  calculated by Zallen is compared to the experimentally determined  $X_c$ .

Since the conductivity is measured along the plane of the film, *i.e.* perpendicular to the main axis of the columns and the amorphous component is located inbetween columns, our result indicate that the higher value corresponds to a percolation of two-dimensional nature; in agreement with  $X_c = 0.45$  calculated by Zallen [4]. Fig. 4 shows the conductivity at room temperature versus  $X$  measured by Raman for the two types of samples, type (a) in solid and type (b) in dashed line. The percolation limit is approximately 0.4 for type (a) and 0.15 for type (b). Type (b) films were prepared in a UHV chamber by evaporation in the amorphous phase and subsequently annealed at various temperatures to produce samples with various values of  $X$ . The volume fraction of crystallinity in type (a) films was obtained by setting the temperature of the substrate above the temperature for which crystallization starts to occur during the growth process. Higher substrate temperatures, above the critical substrate temperature, provided samples with increasing  $X$ . Another way of increasing  $X$  is by the annealing of samples having traces of crystallinity. The annealing temperature in type (a) samples is indicated at the right hand side in Fig. 4.

### *C. Crystallization and preferred orientation*

The crystallization temperatures of silicon and germanium during deposition, ( $T_{sc}$ ) and in amorphous films already formed due to annealing ( $T_c$ ) have been investigated. In the former case, the substrate temperature,  $T_{sc}$ , at which the transition from amorphous to microcrystalline occurs depends on the type of substrate. The substrates investigated were quartz, various types of corning glass, crystalline  $Al_2O_3$ , stainless steel, and quartz slides coated with a thin layer ( $\sim 200 \text{ \AA}$ ) of amorphous

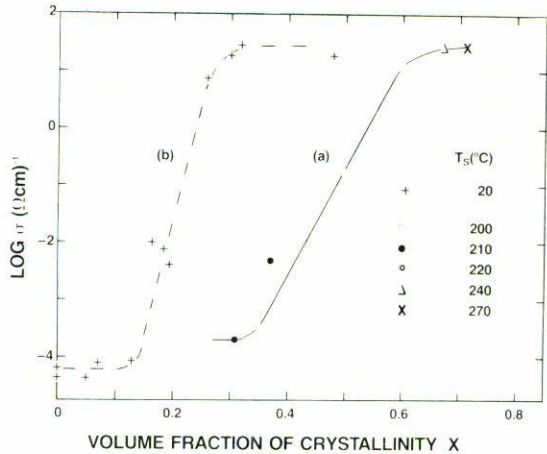


FIGURE 4. Electrical conductivity versus volume fraction of crystallinity for germanium films. Crystallinity was produced by two different ways: by substrate heating (curve a) and by thermal annealing of the amorphous phase (curve b).

silicon prepared at room temperature prior to deposition. The latter substrate will be referred to in this work as amorphous silicon substrates. For both silicon and germanium the lowest  $T_{sc}$  corresponded to films deposited on quartz substrates being  $380^{\circ}\text{C}$  for the former and  $280^{\circ}\text{C}$  for the latter. Those temperatures are substantially lower than the  $T_{sc}$  reported for silicon and germanium films prepared by other techniques [5-7]. Among the investigated substrates the highest  $T_{sc}$  corresponded to films deposited on 7059 corning glass,  $T_{sc} = 450^{\circ}\text{C}$  and  $340^{\circ}\text{C}$  were observed for Si and Ge respectively.

When crystallization is produced by annealing of an amorphous film the crystallization temperature,  $T_c$ , depends on the history of every particular film. If the annealing is performed immediately after deposition under UHV conditions in a film never exposed to air, the crystallization temperature is  $600^{\circ}\text{C}$  regardless of type of substrate and substrate temperature (Fig. 5). However, if the films are exposed to air contamination by removing them from the UHV chamber or by introducing pure oxygen into the chamber, the crystallization temperature increases up to  $700^{\circ}\text{C}$  for films deposited at low substrate temperature. Fig. 5 shows  $T_c$  vs. substrate temperature  $T_s$  for silicon films deposited on quartz and on amorphous silicon annealed in and out the UHV chamber for one hour. The values for  $T_c$  annealed inside UHV are shown with the crosses where the amorphous samples have not been exposed to ambient contamination. Open and closed circles represent  $T_c$  for similar films which have been stored in air at room temperature for few days followed by annealing in a tube furnace flowing with nitrogen.

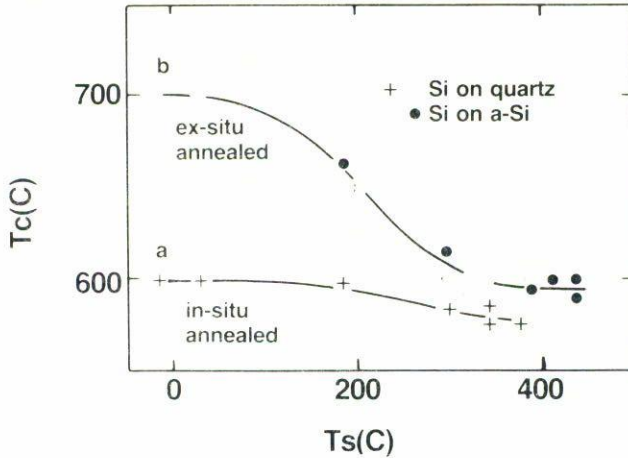


FIGURE 5. Crystallization temperature,  $T_c$  vs. substrate temperature,  $T_s$  of silicon films, for *in-situ* (a) and *ex-situ* (b) annealed.

#### D. Grain-size

In order to study the grain-size, microcrystalline silicon and germanium films were prepared under UHV conditions at  $T_s$  ranging from 20 to 600°C followed by annealing at 800 and 570°C respectively for one hour. The average grain-size of the annealed samples was measured using transmission electron microscopy (TEM). As reported by Herbeke *et al.* [8], the maximum grain-size occurs for  $T_s$  slightly below  $T_{sc}$ . Our results may be explained considering the competition between the homogeneous nucleation at high substrate temperatures and heterogeneous nucleation induced by the chemisorbed foreign species in the voids at low substrate temperatures.

In Fig. 6 we show the grain size dependence on  $T_s$ . Note that there is a maximum for Si at  $T_s = 350^\circ\text{C}$  and at  $T_s = 170^\circ\text{C}$  for Ge. These values correspond approximately to the  $T_{sc}$  for Si and Ge respectively. The maximum for both reaches a few micrometers. Fig. 7 shows the TEM micrographs for Ge at three different values of  $T_s$ , 20, top; 170, middle; and 600°C bottom. the electron diffraction patterns are shown at the upper left corner. The electron diffraction pattern for  $T_s = 170^\circ\text{C}$  is almost that of a single crystal, indicating that the electron beam size is much smaller than the grain size. Returning to Fig. 6, the dash-dot curve refers to annealing under UHV which results in only a slight decrease at  $T_s \leq T_{sc}$ . Since no impurities are present, the grain size is only determined by the annealing conditions. We can also conclude that voids alone do not induce heterogeneous nucleation. For *ex-situ* annealing in the same temperature range ( $T_s < T_{sc}$ ) a drastic reduction in grain size is observed. Again it is the chemisorbed species on the internal surfaces of the voids that promote heterogeneous nucleation causing the reduction in grain size. For  $T_s > T_{sc}$  no voids are present because the material is microcrystalline and therefore the grain size is controlled by homogeneous nucleation.

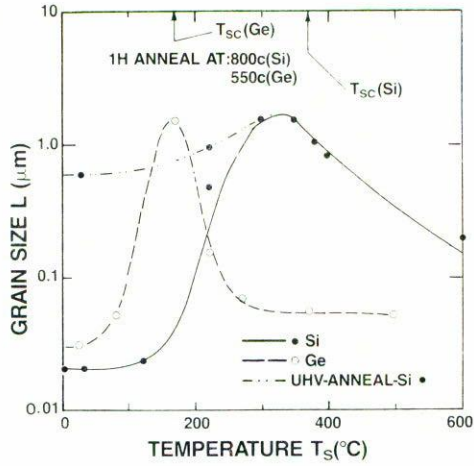


FIGURE 6. Grain size depends on  $T_s$ . The  $T_{sc}$  for silicon and germanium films is indicated. *In situ* and *ex situ* annealings are shown in the figure.



FIGURE 7. Transmission electron micrograph for Ge films prepared at three different substrate temperatures: 20, top; 170 middle; and 600°C bottom.

Parameter	Si
$V_n$	$2 \times 10^{-21} \text{ (cm}^3\text{)}$
$N_0$	$2 \times 10^{22} \text{ (cm}^{-3}\text{)}$
$E_n$	1.35 eV
$V_0/K$	$3.2 \times 10^{-19} \text{ (cm}^3\text{)}$
$f_0$	$8 \times 10^{-22}$
$E_v$	1.77 eV

TABLE I. Parameters for the fit of  $L$  vs.  $T_s$  using Eqs. (4) and (5) and the expression for  $L$ .

In order to understand the appearance of a maximum in  $L$ , we assume that the heterogeneous sites per unit volume,  $N_i$  is proportional to the density of voids, *i.e.*  $N_i = KV_v$ , where  $K$  is the occupation probability per void by chemisorption. If  $V_0$  is the most probable volume of voids [9], the volume fraction,  $f_v$  is given by  $f_v = N_v V_0$ . And  $f_v$  may be taken as

$$f_v = f_{v0} \{1 + f_0^{-1} \exp(-E_v/kT_s)\}^{-1}, \quad (3)$$

with  $f_{v0} = 0.04^{(17)}$ . At high temperatures,  $T_s$  much greater than  $T_{sc}$ ,  $L$  is limited by the number of homogeneous nucleation per unit volume  $N_n$  given by

$$N_n = V_n^{-1} \{1 + N_0^{-1} \exp(E_n/kT_s)\}^{-1}, \quad (4)$$

where  $V_n$  is the minimum volume occupied by a nucleation site [10]. With both competing processes, the grain size  $L = (N_n + N_i)^{-1/3}$ . Table I summarizes the results obtained by fitting this expression to the grain-size  $L$  for Si. The activation energy for homogeneous nucleation  $E_n = 1.35$  eV is much lower than the value 3.7 eV [11] for a-Si already prepared. If we use Shevchik's [9] most probable void volume of  $2.5 \times 10^{-21} \text{ cm}^3$ , the value of  $K$  may be determined, giving approximately 0.01. This means that only approximately 1% of the most probable void density is affected by chemisorption, or alternatively, only 1% of the voids are connected to allow gas molecules to permeate throughout the entire volume.

What we can find from the fit to  $L$  is  $N_i$ , leading to the value of  $N_v$  to within a factor  $K^{-1}$ . Obviously  $K$  depends on the types of gas molecule involved. Thus a careful analysis of the variation of  $L$  enables us to study chemisorption and void structure. For a given gas,  $K$  is constant with  $T_s$ , therefore one can obtain the variations of  $N_v$  with  $T_s$  as shown in Fig. 8. For the UHV annealed, the probability of occupation  $K$  is reduced by a factor of  $10^5$  resulting in a nearly constant  $L$  at low substrate temperature, as shown in the same figure. This substantiates the conclusion that voids alone do not reduce grain-size. This analysis shows that lacking a graingrowth for covalent materials, the grain size is limited by the competition of the homogeneous and heterogeneous nucleation. It is important to recognize that the grain size is affected by the presence of  $N_i$ , 10 orders of magnitude below  $N_0$ .

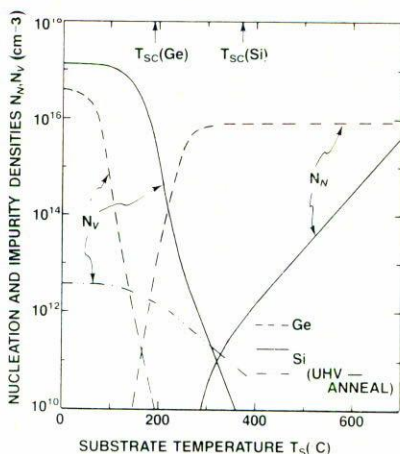


FIGURE 8. Nucleation density  $N_n$  and  $N_i$  vs. substrate temperature for Si and Ge films.

However, three orders of magnitude improvement in vacuum will at most result in a factor of ten increase in  $L$ .

#### 4. Conclusions

In general, for thin film devices, it is desirable to have individual grains with a large aspect ratio (width to thickness). In the present work a systematic study on some of the parameters which affect the nucleation and growth of UHV evaporated silicon and germanium films has been carried out. It is found that by changing the substrate temperature in a range from room temperature to 500°C, silicon and germanium films with crystal structures varying from completely amorphous to highly crystalline are produced. Intermediate substrate temperatures result in films with a diphasic structure, *i.e.* a mixture of amorphous and crystalline phases.

The substrate temperature at which the amorphous to microcrystalline transition occurs for Si and Ge depends on the type of substrate and on the presence of impurities, therefore it is not an intrinsic parameter.

The crystallization temperature of an amorphous film already formed does not depend on either the type of substrate or substrate temperature when annealed *in situ* under UHV conditions. However exposure to ambient contamination before annealing results in an increase in  $T_c$  for films prepared at low substrate temperatures. The latter might be explained by the need to out diffuse the trapped impurities introduced through the voids. Since voids disappear at  $T_s \geq 350^\circ\text{C}$  [12,13], there is no difference between *in situ* and *ex situ* annealing.

The dependence of the grain size on the substrate temperature of Si and Ge films has also been studied. The maximum grain size of the annealed sample occurs when the substrate temperature is in the range in which the deposited film changes

from the amorphous to the crystalline state. These results have been analyzed on the basis of the competition between two nucleation mechanisms, one with and the other without foreign species present.

#### References

1. M. Matsui, Y. Shiraki, and E. Maruyama, *J. Appl. Phys.* **55** (1984) 1590.
2. F. Morin, P. Coissard, and M. Morel, *J. Appl. Phys.* **53** (1982) 3898.
3. H. Richter, Z.P. Wang and L. Ley, *Solid State Comm.* **39**, (1981) 625.
4. R. Zallen, *Fluctuation phenomena*, Ed. E.W. Montroll and J.L. Lebowitz, North-Holland, Amsterdam, (1979) 177.
5. J. González-Hernández and R. Tsu, *Appl. Phys. Lett.* **42** (1983) 90.
6. E.F. Kennedy, L. Csepregi, J. Mayer, and T.W. Sigmon, *J. Appl. Phys.* **48** (1977) 4241.
7. J.E. Green and L. Mei, *Thin Sol. Films.* **37** (1976) 429.
8. G. Herbeke, L. Krausbauer, E.F. Stiegmeier, A.E. Widmer, H.F. Kappert and G. Neugebana, *Appl. Phys. Lett.* **42** (1983) 249.
9. N.J. Shevchik and W. Paul, *J. Noncryst-Solids* **16** (1974) 55.
10. K. Zellama, P. Germain, S. Squeland and J.c. Bourgoïn, *J. Appl. Phys.* **50** (1979) 6995.
11. J. González-Hernández, D. Marin, S.S. Chao and R. Tsu, *Appl. Phys. Lett.* **45** (1984) 101.
12. R. Tsu, D. Martin, J. González-Hernández and S.R. Ovshinsky, *Phys. Rev.* **B35** (1987) 2385.
13. J. González-Hernández, G.H. Azarbayejani, R. Tsu and F.H. Pollak, *Appl. Phys. Lett.* **47** (1985) 1350.

**Abstract.** Se discuten la preparación y caracterización de películas delgadas de silicio y germanio microcristalinas. Se utilizaron varias técnicas de caracterización, tales como medidas eléctricas, espectroscopía Raman, microscopía electrónica de transmisión, difracción de rayos X y microscopía electrónica de barrido. En particular, se discuten la percolación en la conductividad eléctrica y las medidas del tamaño de grano. El efecto más importante que determina las propiedades de estas películas es la presencia de impurezas. Asimismo, para mejorar sus propiedades es necesario un crecimiento controlado bajo condiciones de alto vacío y/o gases de alta pureza en los sistemas de deposición.